

On the Projectile Charge-Sign Dependence of Four-Particle Dynamics in Helium Double Ionization

D. Fischer,¹ R. Moshhammer,¹ A. Dorn,¹ J.R. Crespo López-Urrutia,¹ B. Feuerstein,¹
C. Höhr,¹ C.D. Schröter,¹ S. Hagmann,² H. Kollmus,³ R. Mann,³ B. Bapat,⁴ and J. Ullrich¹

¹*Max-Planck-Institut für Kernphysik, Saupfercheckweg 1, D-69117 Heidelberg, Germany*

²*Institut für Kernphysik, August-Euler Strasse 6, D-60486 Frankfurt, Germany*

³*Gesellschaft für Schwerionenforschung, D-64220 Darmstadt, Germany*

⁴*Physical Research Laboratory, Navrangpura, Ahmedabad-380 009, India*

(Dated: March 31, 2003)

Double ionization of helium by 6 MeV proton impact has been explored in a kinematically complete experiment using a “Reaction Microscope”. For the first time, fully differential cross sections for positively charged projectiles have been obtained and compared with data from 2 keV electron impact. The significant differences observed in the angular distribution of the ejected electrons are attributed to the charge-sign of the projectile, resulting in different dynamics of the four-particle Coulomb-system, which is not considered in the first Born approximation.

PACS numbers: 34.10.+x, 34.50.Fa

Helium double ionization resulting from the interaction with time-dependent external forces belongs to the most simple and, thus, fundamental dynamical many-electron problems in atomic physics. Whereas single ionization of helium in most cases can be explained by the interaction of the projectile with a single active target electron, which moves in a screened nuclear Coulomb potential, in double ionization the correlation between the two electrons in the final and the initial state, as well as during the interaction, is of decisive importance. Hence, there are numerous studies to explore helium double ionization by particle and antiparticle impact, by single photons as well as in intense laser fields (for a recent overview see [1] and various articles in [2]).

For charged particle impact, the interest was focussed on the study of the total single (σ^+) and double (σ^{++}) ionization cross sections mainly by exploring their ratio $R = \sigma^{++}/\sigma^+$ (Fig. 1). Investigations strongly concentrated on two rather general observations: First, a limit at high velocities has been found, where the ratio R becomes completely independent of the charge Z_P and velocity v_P of the projectile. This limit, reached at different v_P for various particles, has been established experimentally for collisions with electrons [3, 4], positrons [5], protons, antiprotons [6, 7] and highly charged ions up to Ne^{10+} [8]. Second, at intermediate and low projectile velocities, where R has a strong dependence on v_P , a distinct difference in R has been found for collisions with positively and negatively charged particles. Well above threshold for electron and positron impact (at velocities $v_P \gtrsim 8$ a.u.), this difference becomes independent of the projectile mass and, thus, is a pure charge effect.

The general behavior of the ratio R has been first explained by McGuire [9], who distinguished between two mechanisms for double ionization: “shake-off” (SO) and “two-step 2” (TS2). The shake-off dominates in the high velocity regime. Here, one electron is ionized directly

by the projectile, described by the first Born approximation (FBA) where the cross section scales like $(Z_P/v_P)^2$. Double ionization only occurs due to the rearrangement of the remaining target electron as a result of the “sudden” change in the electronic screening of the nuclear charge. This effect is independent of the charge and velocity of the incident projectile and, therefore, R reaches a constant value. At lower velocities, the TS2-mechanism prevails, where the electrons are ejected sequentially via two single interactions with the projectile, corresponding to a second order effect. Treating both electrons independently, the double ionization cross section becomes proportional to $(Z_P/v_P)^4$ and, thus, R scales like $(Z_P/v_P)^2$.

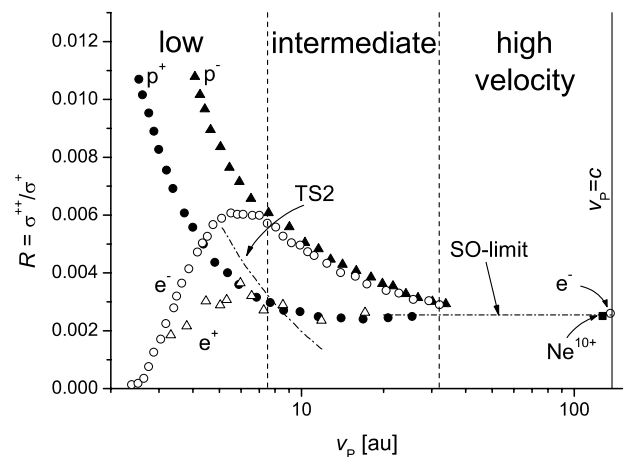


FIG. 1: The ratio $R = \sigma^{++}/\sigma^+$ of the total double-to-single ionization cross sections for helium as a function of the projectile velocity for protons (full circles [6]), antiprotons (full triangles [6, 7]), electrons (open circles [3, 4]), positrons (open triangles [5]) and Ne^{10+} (full square [8]). The dash-dotted lines denote the velocity dependence for the “pure” two-step 2 (TS2) mechanism and the high-velocity limit for shake-off (SO) [9].

The difference between positive and negative projectiles was ascribed to an interference between the SO and the TS2 amplitude resulting in a $(Z_P/v_P)^3$ contribution in the double ionization cross section.

Theoretically, in a more complete picture that has been developed later on, not only SO and TS2 but also other electron-electron correlation processes, e.g. two-step 1 [1], have to be taken into account. Including electronic correlations, the high-velocity limit of R has been described in good agreement with the experimental results by Ford and Reading [10] in a first Born calculation. At low and intermediate projectile velocities, R has been successfully predicted within the forced impulse method (FIM) (e.g. [11]) for protons and antiprotons. Here, the electronic correlations are included by projecting, after short time intervals, independently evolving electrons on correlated states. The differences in R for antiprotons and protons also have been reproduced in classical calculations (CTMC) by Olson [12] and most recently by Morita et al. [13]. In the classical picture, the dependence of R on the sign of the projectile charge has been explained by the different collision dynamics. Theoretical fully differential double ionization cross sections, however, have never been reported in the literature for positively charged particle impact until now.

Experimentally, only a few kinematically complete experiments on helium double ionization have been reported in the perturbative regime (100 MeV/u C^{6+} -projectiles [14]) as well as in a strongly non-perturbative situation (3.6 MeV/u Au^{53+} -projectiles [15]). However, all of these experiments suffered from the statistical quality of the data, prohibiting the extraction of more than double differential cross sections. For electron impact, the so-called (e,3e) reactions, fully differential data have been available for several years for projectile energies from 500 eV to 5.6 keV [16–20]. Theoretical calculations, in particular the convergent close-coupling (CCC) method, were able to describe the fully differential (e,3e) spectra over a broad range of momentum transfers and energies of the ejected electrons [20–22].

In this Letter, we report on the first fully differential experimental cross sections for helium double-ionization by positively charged projectiles in comparison with earlier data for electron impact [20, 22] in order to ultimately explore the dynamics of the sign-dependent differences in R and identify possible interferences or other contributions between first and second order Born amplitudes. We have chosen intermediate velocities of 12.2 a.u. and 15.5 a.u., respectively. Here, the difference in R for positively and negatively charged particle impact is still large, close to a factor of two, whereas the mass-dependent difference is already negligibly small.

The experiment has been performed using a multi-electron recoil-ion momentum spectrometer (“reaction microscope”) which has been described in detail elsewhere [23]. In short, a well-collimated (1 mm \times 1 mm),

pulsed (pulse length \approx 1 ns, repetition rate = 680 kHz) proton beam (beam current = 500 pA, i.e. about 5000 protons per pulse) from the Tandem accelerator at the Max-Planck-Institute (MPI) in Heidelberg with an energy of 6 MeV ($v_P=15.5$ a.u.) was used to ionize cold helium atoms provided by a supersonic gasjet in the reaction microscope. The ejected electrons and the recoiling ion were extracted in opposite directions along the beam axis by a weak electric field (2.3 V/cm) and were detected by two-dimensional position sensitive multichannel plates. In addition, to confine the motion of the electrons with a large transverse momentum (with respect to the beam axis), a uniform magnetic field of 14 G was applied oriented along the incoming beam direction. In this way, all electrons with energies below 25 eV were forced onto the detector in a spiral motion and were detected with the full solid angle of 4π . Since the momenta of both the electrons have to be determined to obtain the full information of the final state momentum space in a double ionization event, a “multihit” capable delayline anode (dead-time \approx 10 ns) was used for the electron position readout. From the measured position on the detector and the time-of-flight, the trajectories of the extracted particles were reconstructed and their initial momenta were calculated. One week of continuous beam-time was required to observe 200 000 double ionization events and, thus, to have a sufficient amount of data to extract fully differential cross sections.

The achieved momentum resolution for the He^{2+} ions was $\Delta p_{R\parallel} = 0.1$ a.u. in the longitudinal and $\Delta p_{R\perp} = 0.3$ a.u. in the transverse direction, respectively. The electron longitudinal momentum resolution is approximately $\Delta p_{e\parallel} = 0.01$ a.u. Stating the transverse electron momentum resolution is more complicated due to the cyclotron motion of the electrons in the magnetic field. It depends on both the longitudinal and the transverse momentum of the electron and, on the average, it is about 0.1 a.u. The longitudinal and transverse momenta determine the polar angle resolution of the electrons, i.e. the angle with respect to the beam direction.

In figure 2, the fully differential cross sections are shown and compared to the electron impact data. A coplanar geometry is chosen, i.e. the momenta of the electrons as well as the incoming and outgoing momentum vectors of the projectile are laying in the same plane (within an angular window $\pm 30^\circ$). The density plots represent the angular distribution of both electrons with respect to the projectile beam direction for low (0.2–0.8 a.u.), intermediate (0.8–1.4 a.u) and large (1.4–2.0 a.u.) momentum transfer and for an equal sharing of the excess energy ($\Delta E_{e1,e2} < 2.5$ eV). The angle of the momentum transfer vector ranges from 0–85 degrees. In spite of long beam-times, the statistical quality of the data required the integration over electron energies from 0 to 25 eV. Even though the statistical quality of the electron impact data is somewhat better, identical projec-

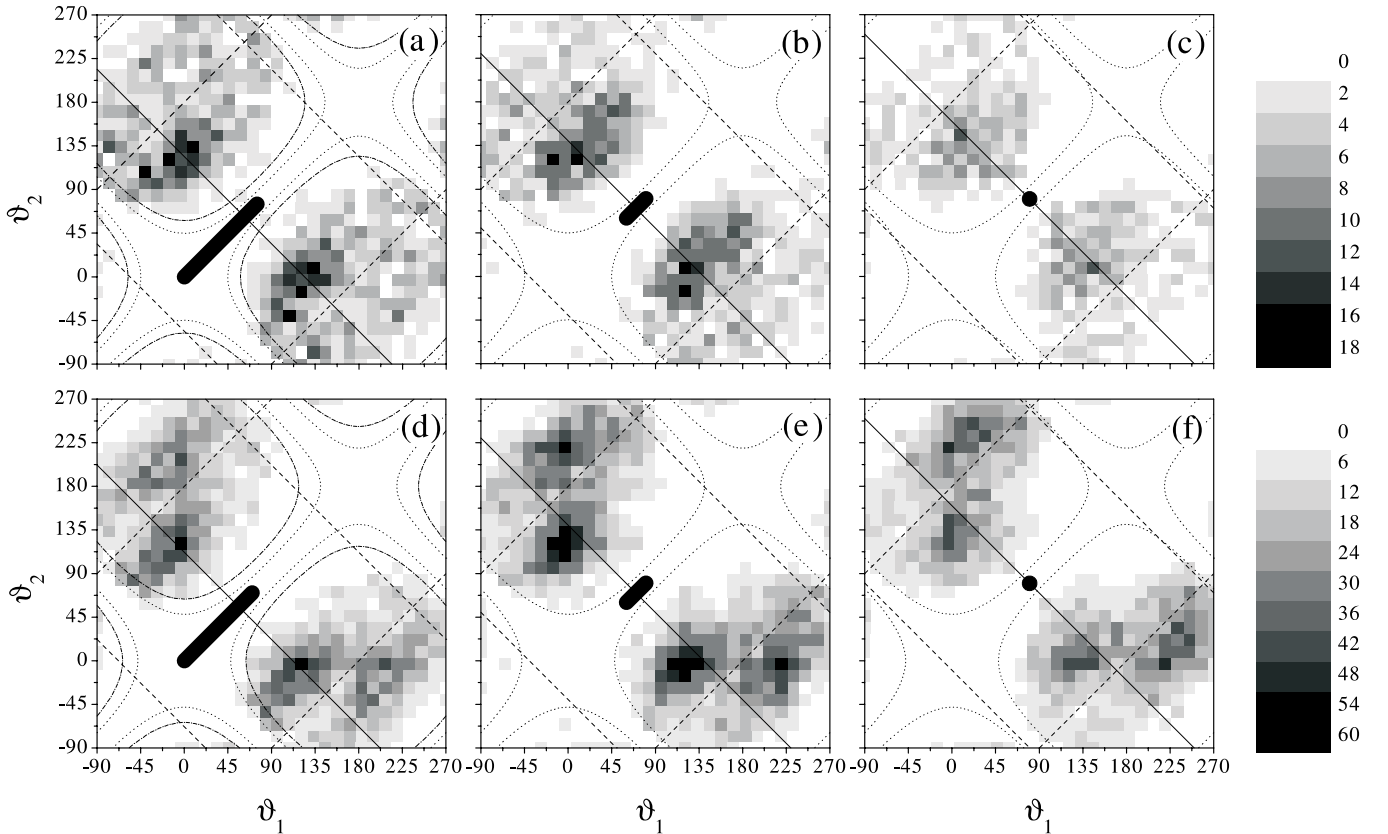


FIG. 2: Angular distribution of the two ejected electrons (ϑ_1, ϑ_2 : polar angle with respect to the forward beam direction) in coplanar geometry for proton (a-c) and electron (d-f) impact at a momentum transfer of 0.2 to 0.8 a.u. (a, d), 0.8 to 1.4 a.u. (b, e) and 1.4 to 2.0 a.u. (c, f), respectively. A symmetric energy sharing is chosen ($E_{e1} = E_{e2} < 25$ eV). The black area in the middle of the diagrams denotes the kinematically allowed momentum transfer directions, which ranges from about 0 to 75 degrees (a, d), 60 to 80 degrees (b, e) and 75 to 85 degrees (c, f), respectively. The symmetry axis obtained in the FBA (solid lines) and the nodes for dipole transitions (dashed lines) are shown for an averaged momentum transfer angle.

tions and conditions have been used for the comparison. The dead time of the electron detector causes a limitation of the angular acceptance of the spectrometer, which depends on the energy of the ejected electrons, and, thus, the acceptance has to be calculated for all energies separately. Exemplarily, dotted and dash-dotted lines enclose the angular range for electrons with 5 eV (Fig. 2 (a) and (d), dash-dotted lines) and with 20 eV (Fig. 2, dotted lines) that is not affected by the limited acceptance.

All six diagrams feature a clear four-peak structure. Since for an equal energy sharing the electrons are interchangeable, the spectra are mirrored at the diagonal line from the lower left corner to the upper right and the two peaks in the upper left are equivalent to those in the lower right. As discussed in detail in Ref. [20], the four-peak structure in essence results from dipole selection rules along with post-collision repulsion between the two electrons. Whereas the latter pushes the electrons away from the diagonal, dipole selection rules in their strict form would enforce zeros along the dashed lines. Thus, we observe a clear signature of dipole contributions under the kinematical conditions chosen in Fig. 2 for both

projectile charge states.

Furthermore, in comparison with single ionization, the structures can be identified as “binary” and “recoil peak”, which are well established for electron and ion (e.g. [24, 25]) impact. The peaks that are closer to the middle of the diagrams represent the situation that the sum of both electron momenta points in the direction of the momentum transfer, in accordance with the binary peak in single ionization. In the equivalent way, the two remaining peaks correspond to the recoil peak, where the sum of the electron momenta is directed opposite to the momentum transfer, i.e. both electrons are scattered in the same direction as the projectile and the recoil ion compensates the momenta of all three other particles.

Significant differences can be observed for proton and electron impact. First, the relative intensity of binary to recoil-peak is always larger for proton impact, most pronounced for larger momentum transfers or, vice versa, the recoil-peak is clearly more intense for electron impact. This feature has been found recently for single ionization as well [26], where theoretical triply differential cross sections were compared for positively and neg-

atively charged particle impact. As a second difference, for electron impact a strong asymmetry appears with respect to the momentum transfer direction, which is defined by the fixed kinematical conditions and is indicated by the thick bars in the diagrams. For proton collisions, the symmetry in the angular distribution enforced by the first Born theory is instead closely fulfilled; the solid lines in Fig. 2 represent the symmetry axis.

The differences observed in the spectra might be interpreted on the basis of the classical calculations mentioned in the introduction: At not too large impact parameters, negatively charged projectiles tend to push one electron towards its parent atom, such that the interaction of the electrons with the target nucleus as well as the direct mutual electron-electron interaction (TS1) might become more important. A closer look at the asymmetry in the electron data clearly shows that, even here, the binary peak is close to the first Born symmetry condition. Only the recoil peak strongly breaks the symmetry. Here, strong “higher order effects”, i.e. interactions with the second electron as well as with the target nucleus, are expected. Accordingly, a positively charged projectile tends to pull one electron away from the parent nucleus and “shaking” the second one into the continuum, thereby increasing the probability of a “clear” binary peak. Within such a scenario, it is evident that dynamic electron-electron interaction during the collision, like TS1, where the first electron interacts with the second one, might be much less important.

In a perturbative quantum mechanical description, the total and differential cross sections are given by the Born series $\sigma = \alpha_1 Z_P^2 + \alpha_2 Z_P^3 + \alpha_3 Z_P^4 + \dots$, where the only difference between positively and negatively charged projectiles is the sign of the Z_P^3 -term. However, it is surprising that the higher order terms that lead to an asymmetry with respect to the momentum transfer direction in the patterns for electron impact do not result in a similar asymmetry for proton collisions. In a previous semiempirical study [27], the faster convergence of R for proton collisions has been attributed to the cancelation of the total Z_P^3 and Z_P^4 contributions. Nevertheless, there is no evident physical reason why these two terms should be of the same magnitude and add to zero for proton impact. It is even more surprising that, also for the fully differential cross sections in proton collisions, the Z_P^3 - and Z_P^4 -term cancel each other or, at least, add to a symmetric angular distribution, which is the only possible explanation of the observed symmetry. The cancelation of the higher order terms not only for the integrated cross section, but also for the fully differential data, would be a clear indication that, in general, all contributions beyond the first Born approximation are of less importance in collisions with positively charged projectiles.

In conclusion, for the first time, fully differential cross sections for the double ionization of helium by proton impact have been measured over a large range of final state

momentum space. Comparison of the data with those for electron impact at a similar collision velocity reveals significant differences. These differences have been assigned to the projectile charge-sign dependence of the cross sections in the Born series and were qualitatively interpreted as a result of the different collision dynamics for negatively and positively charged projectiles. Clearly, a more detailed understanding of the four-body collision dynamics requires theoretical approaches that go beyond a first order approximation delivering fully differential cross sections. Moreover, for lower velocities, where the cross sections become projectile mass dependent, proton and antiproton induced double ionization data are urgently required.

We acknowledge the excellent work of the MPI accelerator staff for the preparation of the ion beam. This work was supported from the GSI, BMBF, and the DFG within the Leibniz-Program. We want to thank A. Voitkiv and T. Kirchner for the fruitful discussions.

-
- [1] J. H. McGuire, *Electron Correlation Dynamics in Atomic Collisions* (Cambridge University Press, 1997).
 - [2] J. Ullrich and S. Shevelko, *Many Particle Quantum-Dynamics in Atomic and Molecular Fragmentation* (Springer-Verlag, Berlin, 2003), in press.
 - [3] B. L. Schramm, A. J. H. Boerboom, and J. Kistemaker, *Physica* (Utrecht) **32**, 185 (1966).
 - [4] A. Müller, et al., *J. Phys. B* **16**, 2039 (1983).
 - [5] M. Charlton, et al., *J. Phys. B* **21**, L545 (1988).
 - [6] L. H. Andersen, et al., *Phys. Rev. Lett.* **57**, 2147 (1986).
 - [7] L. H. Andersen, et al., *Phys. Rev. A* **40**, 7366 (1989).
 - [8] J. Ullrich, et al., *Phys. Rev. Lett.* **71**, 1697 (1993).
 - [9] J. H. McGuire, *Phys. Rev. Lett.* **49**, 1153 (1982).
 - [10] A. L. Ford and J. F. Reading, *J. Phys. B* **21**, L685 (1988).
 - [11] A. L. Ford and J. F. Reading, *J. Phys. B* **27**, 4215 (1994).
 - [12] R. E. Olson, *Phys. Rev. A* **36**, 1519 (1987).
 - [13] S. Morita, N. Matsuda, N. Toshima, and K. Hino, *Phys. Rev. A* **66**, 042719 (2002).
 - [14] B. Bapat, et al., *J. Phys. B* **33**, 1437 (2000).
 - [15] A. N. Perumal, R. Moshhammer, M. Schulz, and J. Ullrich, *J. Phys. B* **35**, 2133 (2002).
 - [16] I. Taouil, A. Lahmam-Bennani, A. Duguet, and L. Avaldi, *Phys. Rev. Lett.* **81**, 4600 (1998).
 - [17] A. Lahmam-Bennani, et al., *Phys. Rev. A* **59**, 3548 (1999).
 - [18] A. Dorn, et al., *Phys. Rev. Lett.* **82**, 2496 (1999).
 - [19] A. Dorn, et al. (2003), submitted.
 - [20] A. Dorn, et al., *Phys. Rev. Lett.* **86**, 3755 (2001).
 - [21] A. Kheifets, et al., *J. Phys. B* **32**, 5047 (1999).
 - [22] A. Dorn, et al., *Phys. Rev. A* **65**, 032709 (2002).
 - [23] R. Moshhammer, et al., *Nucl. Instrum. Methods Phys. Res. B* **108**, 425 (1996).
 - [24] H. Ehrhardt, M. Schulz, T. Tekaas, and K. Willmann, *Phys. Rev. Lett.* **22**, 89 (1969).
 - [25] M. Schulz, et al., *J. Phys. B* **34**, L305 (2001).
 - [26] A. Voitkiv, B. Najjari, and J. Ullrich, submitted (2002).
 - [27] L. H. Andersen, et al., *Phys. Rev. A* **36**, 3612 (1987).